Peer-reviewed version available at *Catalysts* **2018**, *8*, 634; doi:10.3390/catal8120634

Recent Progress in Constructing Plasmonic Metal/Semiconductor Hetero-nanostructures for Improved Photocatalysis

Liang Ma [a*], Shuang Chen [a], You-Long Chen [a], Mo-Xi Liu [a], Hai-Xia Li [a], Yi-Ling Mao [a], Si-Jing Ding [b*]

[a] School of Science, Wuhan Institute of Technology, Wuhan, 430205, P. R. China.

[b] School of Mathematics and Physics, China University of Geosciences (Wuhan), Wuhan 430074, Wuhan, P. R. China.

[*] Corresponding author E-mail: maliang@wit.edu.cn (L. M.); dingsijing@cug.edu.cn (S. J. D)

Abstract

Hetero-nanomaterials constructed by plasmonic metals and functional semiconductors show enormous potential in photocatalytic applications, such as water splitting, hydrogen production, CO_2 reduction, pollutants treatment. Their photocatalytic performances can be better regulated through adjusting structure, ingredient, and components arrangement. Therefore, the reasonable design and synthesis of metal/semiconductor hetero-nanostructures is of vital significance. In this article, we briefly review the recent progress in efficiently establishing metal/semiconductor nanomaterials for improved photocatalysis. The defined photocatalysts mainly include traditional binary hybrids, ternary multi-metals/semiconductor and metal/multi-semiconductors heterojunctions. The underlying physical mechanism for the improved photocatalytic activity of the established photocatalysts are highlighted. At the end of this article, a brief summary and possible future perspectives for further development in this field are demonstrated.

Keywords: photocatalysis; plasmon; metal/semiconductor; electron transfer; energy conversion

Peer-reviewed version available at Catalysts 2018, 8, 634; doi:10.3390/catal8120634

1. Introduction

The increasing energy crisis and environmental pollution are common problems faced by the world in the twenty-first century, the whole world is seeking ways to ease these issues. As a sustainable and clean way to convert solar energy, semiconductor-based photocatalysis has been intensely investigated and widely used in energy store and pollutant treatment. [1-10]. Since Fujishima and Honda firstly applied TiO_2 electrode to electrochemical water splitting under ultraviolet light irradiation in 1972 [11], large amounts of semiconductor materials have been extensively explored for photocatalytic applications, such as organic degradation, hydrogen production, CO_2 reduction. [12-18]. In the case of photocatalytic process, semiconductor can absorb sunlight when the energy of the incident photons is equal or larger than its band gap. However, the commonly used semiconductors often have wide band gaps, indicating that they can only be excited by ultraviolet light [19-20]. As the semiconductor is excited by incident light, the formation of photogenerated electron-hole pairs occurs. While, the fast the recombination of electron-hole pairs in semiconductor plays a negative role on the photocatalytic reaction. Therefore, to optimize the photocatalytic activity of semiconductor, the development of new strategies to expand the light response region and speed up the separation rate of electron-hole pairs is necessary.

Over the past two decades, metal nanocrystals have attracted intense research attention due to their extraordinary physical and chemical characteristics [21-23]. The most fascinating property of metal nanocrystals is their plasmonic optical peculiarity. Plasmon resonance of metal nanomaterials refers to the collective oscillations light-excited free charges, which can endow metal nanocrystals with strong light absorption and scattering cross-sections [24-30]. Furthermore, the localized surface plasmon resonance excitation of a metal nanoparticle can induce strong local electromagnetic field. Moreover, upon resonant excitation, plasmonic metal nanocrystals interact strongly with light, the oscillation of free electrons quickly dephase and lead to the generation of energetic hot electrons and holes. Only certain metal nanocrystals, such as Au, Ag, Cu, Al, possess noticeable surface plasmon resonance [31-34]. The plasmon

Peer-reviewed version available at Catalysts 2018, 8, 634; doi:10.3390/catal8120634

resonance of these metal nanomaterials can be easily adjusted through varying the sizes and morphologies, which could across the entire visible spectrum [35-40]. With these characters, the plasmonic metals deservedly display great promises for the effective solar energy conversion in photocatalytic reaction.

Incorporating plasmonic metal nanocrystals with semiconductor photocatalysts to form metal/semiconductor hybrid nanostructures is a potential way to enhance the light absorption, charge generation and separation in the photocatalytic process. Great efforts have been applied to construct various metal/semiconductors hybrids with excellent photocatalytic performance [41-45]. In present article, we give a brief review about the recent efforts in efficient preparation of metal/semiconductor nanomaterials for improved photocatalytic applications. The defined photocatalysts are mainly centralized in traditional binary hybrids, ternary multi-metals/semiconductor and metal/multi-semiconductors heterojunctions. The underlying physical mechanism (including plasmon coupling of multi-metals, co-catalytic effect of functional metals, plasmon-mediated Z-scheme and p-n heterojunctions of multi-semiconductors) for the efficiently improved photocatalysis of metal/semiconductor heterojunctions are highlighted. In the end, a brief summary and discussion on the future challenges in the area of metal/semiconductor photocatalysis are demonstrated.

2. Binary Metal/Semiconductor Hybrids for Enhanced Photocatalysis

Binary photocatalysts constructed by one plasmonic metal and one semiconductor are the most frequently studied. In metal/semiconductor heterojunction, plasmon can modulate photocatalysis mainly through the following characteristics: 1) strong light absorption and scattering; 2) large local electromagnetic field; 3) abundant hot electrons generation [46-50]. Thus, in the photocatalytic process, plasmon could promote the redox reaction via following pathways: enlarging light trapping, speeding charge separation, plasmon-induced energy transfer, and hot electron injection [51-55]. Since the optical and photocatalytic performances of metal/semiconductor hybrids are highly depended on their morphologies and structures, the design of hetero-nanostructure is very important. In this section, we mainly focus on the recent progress about the

Peer-reviewed version available at Catalysts 2018, 8, 634; doi:10.3390/catal8120634

structural adjustment of binary metal/semiconductor photocatalysts. Traditional core-shell, yolk-shell and anisotropic morphologies are highlighted. The underlying enhanced mechanism for photocatalysis of the classified nanostructures is demonstrated.

Typical core-shell structural motif of metal/semiconductors has special advantages for photocatalytic reaction, such as maximizing the active interface and protecting the core metal [56-61]. Recently, Zhang and his co-workers reported the preparation of high-quality Au@CdS core-shell hybrids with atomically organized interfaces [62]. As shown in Figure 1 a and b, the high-yield and monodisperse Au@CdS with quasi-single crystalline shell were observed. The photocatalytic activity of Au@CdS was evaluated by hydrogen evolution. The results indicated that Au35@CdS5 which the Au core size was maintained around 35 nm and CdS shell thickness was 5 nm exhibited highest activity with the rate reaching to 24.0 mmol g^{-1} h^{-1} (see Figure 1c). The femtosecond transient absorption testing indicated that the unique interfacial features enabled highly efficient hot electron injection from Au core to semiconductor shell.

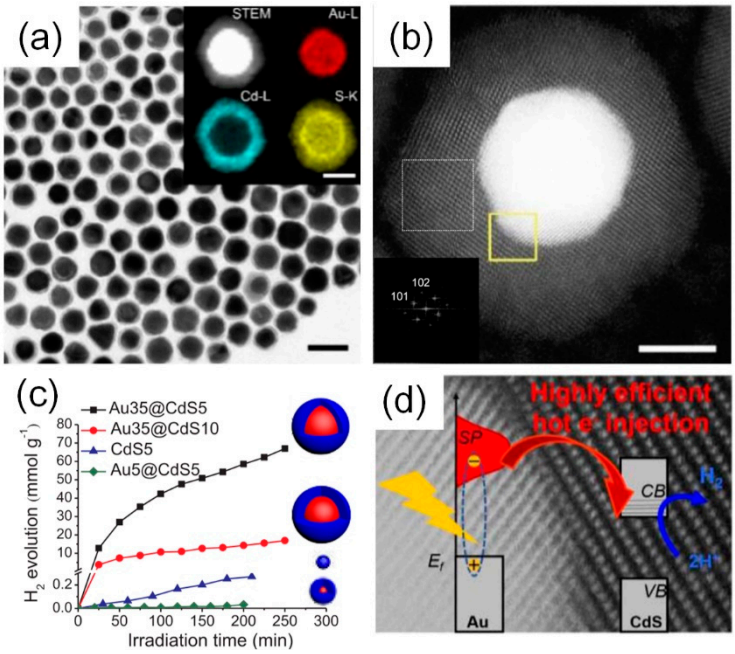

Figure 1. (**a**) and (**b**) Morphology characterization of prepared Au@CdS nanocrystals. Scale bar in (**a**) and (**b**) are 20 nm and 10 nm, respectively. (**c**) Photocatalytic hydrogen evolution activities of prepared spherical Au@CdS with different structural characteristics in comparison with pure CdS under visible light irradiation. (**d**) Schematic illustration of the efficient hot electron-mediated

Peer-reviewed version available at Catalysts 2018, 8, 634; doi:10.3390/catal8120634

photocatalysis that is facilitated by the atomically organized interface between Au core and CdS shell. Copyright 2018 Elsevier.

Apart from core-shell nanostructures, metal-semiconductor yolk-shell nanostructure also benefits for photocatalysis. The unique void between metal and semiconductor could efficiently improve light trapping and accelerate plasmon-induced resonant energy transfer [63-66]. For example, Han and co-workers reported a yolk-shell nanostructure consisting of plasmonic Au nanorod yolk and CdS shell [67]. The synthetic route was shown in Figure 2a, the most important point in the process was the action exchange. The identified yolk-shell structure of Au/CdS was given in Figure 2b. The prepared Au-CdS yolk-shell hybrids exhibited significantly enhanced activity for photocatalytic hydrogen evolution under visible light (λ > 400nm) irradiation in comparison to CdS hollow nanoparticles, Au@CdS core-shell nanostructures (see Figure 2c). The synergism between multiple photon reflections rendered by the yolk-shell structure and the radiative relaxation of plasmon energy were thought to be the promotional effect for the photocatalysis, which were proposed in Figure 2d.

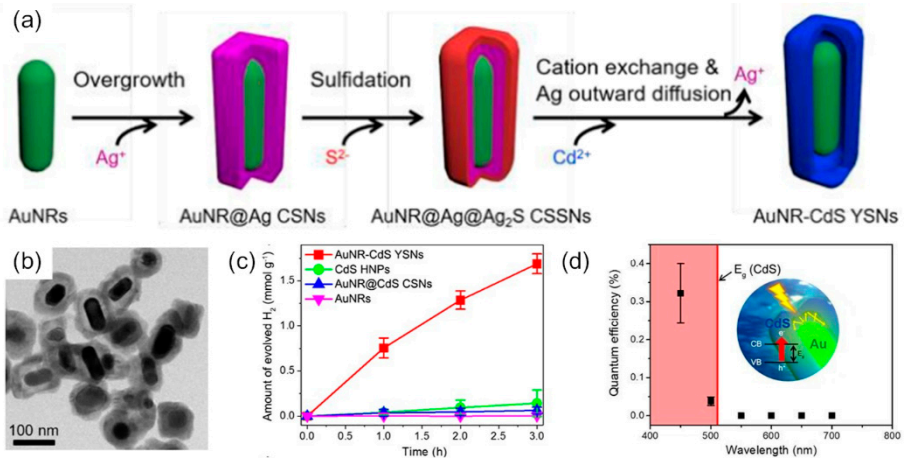

Figure 2. (**a**) Schematic illustrating the synthesis route of Au-CdS yolk-shell nanostructures. (**b**) Transmission electron microscopy (TEM) image of Au-CdS yolk shell nanostructures. (**c**) Amounts of hydrogen evolved during the photocatalysis with different catalysts, which were normalized to the total mass of catalysts. (**d**) Hydrogen evolution activity of Au-CdS yolk-shell hybrids as a function of excitation wavelength. Inset shows the schematic illustration of the synergism. Copyright 2018 Royal Society of Chemistry.

Peer-reviewed version available at Catalysts 2018, 8, 634; doi:10.3390/catal8120634

In addition, anisotropic binary metal/semiconductor hybrids have unique merits for photocatalytic reaction. By selective growing semiconductor shells on the surface of metal nanocrystals, the processes of electron injection and energy transfer can be prominently accelerated [68-70]. In 2016, Stucky's group prepared an anisotropic Au/TiO_2 nanodumbbell, which the TiO_2 nanoshells was spatially grown at the two ends of Au nanorod (see Figure 3a) [71]. Through testing the hydrogen production by evaluating the photocatalytic degradation of methanol, the designed Au/TiO_2 shown best photocatalytic activity (see Figure 3b). As proposed in Figure 3c, for the nanodumbbells, the oxidation pathway occurs on their side surface, when lateral side of Au can be directly exposed to electron donors. With Au partially exposed, Au could generate a concentrated electromagnetic field that focus energy flux around the semiconductor, and thus enhancing hot-electron generation and photocatalytic activity.

Similarly, Han and co-workers reported a rational synthesis strategy for the realization of plasmonic metal-semiconductor heteronanocrystals with intended configurations through the site-selective overgrowth of semiconductor Cu_2O on desired sites of anisotropic Au nanocrystals [72]. The morphology characterization in Figure 3d clearly shown that the Cu_2O were grown on the vertices of hexoctahedral Au (Au_{vertex}-Cu_2O). The Au_{vertex}-Cu_2O exhibited outstanding photocatalytic activity for hydrogen production relative to the other nanostructures. A series of experiments (including adding insulating layer and theoretical simulation) indicated that the efficient charge separation by strong plasmon excitation, subsequent sustainable hot electron transfer and plasmon energy transfer process (1 and 2 labeled in Figure 3f) were responsible for the enhanced photocatalytic activity.

Peer-reviewed version available at Catalysts 2018, 8, 634; doi:10.3390/catal8120634

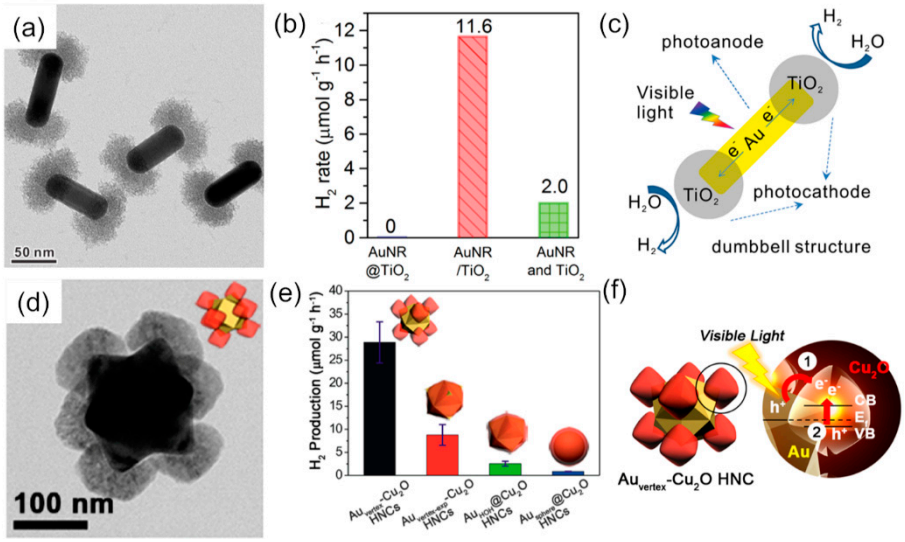

Figure 3. (**a**) TEM image of Au/TiO_2 nanodumbells. (**b**) Hydrogen evolution rate by various catalysts. (**c**) Structure and mechanism of operation under visible light of individual Au/TiO_2 dumbbell. Copyright 2016 American Chemical Society. (**d**) TEM image of Au_{vertex}-Cu_2O heteronanocrystal. (**e**) Photocatalytic hydrogen generation rates of different heteronanocrystals. (**f**) Schematic illustration of possible plasmon-induced charge separation processes for Au_{vertex}-Cu_2O. Copyright 2016 American Chemical Society.

4. Plasmon Coupling, Co-Catalytic Effect, and Components Arrangement in Ternary Multi-Metals/Semiconductor Catalysts

Integrating one metal nanocrystal with binary metal/semiconductor to form ternary hetero-nanostructure could dramatically improve the photocatalytic activity due to the synergistic effect between the three nano-spaced components [73-74]. The introduced metals could be a plasmonic donor or functional catalyst. In that way, the synergistic effect includes plasmon coupling and co-catalytic effect. Furthermore, the arrangements of the three different components also influence the whole photocatalytic performance. In this section, we focus on the progress achieving in constructing ternary multi-metals/semiconductor photocatalysts. The excellent photocatalytic performances of defined nanomaterials and underlying physical mechanism are highlighted.

The plasmon coupling between two metals could generate excellent optical properties. The strong coupling induced broad resonance region can largely enhance the light trapping [75-76]. Simultaneously, the coupled local electric field can

Peer-reviewed version available at Catalysts 2018, 8, 634; doi:10.3390/catal8120634

efficiently accelerate the hot electron generation and suppress the recombination of electron-hole pairs [77-78]. Recently, Huang and co-workers used Au-Ag bimetallic nanoparticles to modify ZnO nanorods via simple photo-deposition procedure (see Figure 4a) [79]. The photocatalytic tests indicated that ZnO co-decorated by 0.8 wt% Au-Ag exhibited best photocatalytic ethylene-oxidation activity. The possible mechanism of the excitation of surface plasmon and electron transfer process was shown in Figure 4b, the cooperative action of plasmonic Au-Ag alloys induced large visible-light absorption and efficient carrier separation were thought to be the enhanced factor.

Besides, Kamimura et. al synthesized (core@shell)@shell ((Au@Ag)@Au) nanoparticles by a multistep citrate reduction method for utilization as photosensitizers of TiO_2 (see Figure 4c) [80]. They confirmed that (Au@Ag)@Au/TiO_2 could oxidize 2-propanol into acetone and CO_2 under visible light irradiation, and its acetone evolution rate was approximately 15-times higher than that of Au/TiO_2. They proposed that the excited electrons in the (Au@Ag)@Au were injected into the conduction band of rutile TiO_2, and then the electron-deficient (Au@Ag)@Au could oxidize 2-propanol into acetone and CO_2.

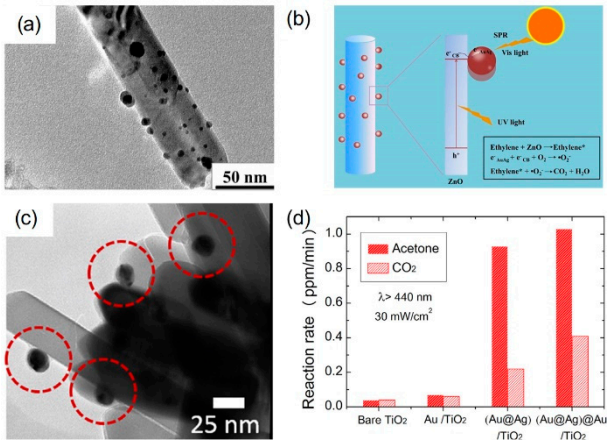

Figure 4. (**a**) TEM image of AuAg/ZnO. (**b**) Pictographic representation and the possible mechanisms of the excitation of surface plasmon and electron transfer process Copyright 2017 Elsevier. (**c**) TEM image of (Au@Ag)@Au decorated TiO_2. (**d**) Acetone and CO_2 evolution rates of 2-propanol decomposition over the contrast samples under visible light irradiation. Copyright 2017 Elsevier.

Preprints (www.preprints.org) | NOT PEER-REVIEWED | Posted: 21 November 2018 doi:10.20944/preprints201811.0523.v1

Peer-reviewed version available at Catalysts 2018, 8, 634; doi:10.3390/catal8120634

As a functional metal, Pt nanocrystal is an ideal catalyst for oxygen reduction reaction due to its suitable Fermi level and excellent ability for trapping electrons [81-83]. Pt nanocrystal is commonly used as effective co-catalyst and active site. It can be decorated onto the surface of a semiconductor for improved photocatalysis. Combine Pt with plasmonic metal/semiconductor hetero-nanostructures can extremely boost the redox reaction [84-86]. In 2015, Moskovits' group fabricated a device including both Au nanorod, TiO_2 and Pt to achieve panchromatic photoproduction of hydrogen [87]. Firstly, Au nanorods were dropped cast on quartz slides forming a dense layer with panchromatic absorption. Then TiO_2 film was deposited and acted as a hot electron filter, and Pt nanoparticles were capped functioning as the hydrogen evolution catalyst (see Figure 5a). The photocatalytic results revealed that the sample with Au nanorods of aspect ratio 1.4 and 3.0 shown highest photocatalytic activity for hydrogen production.

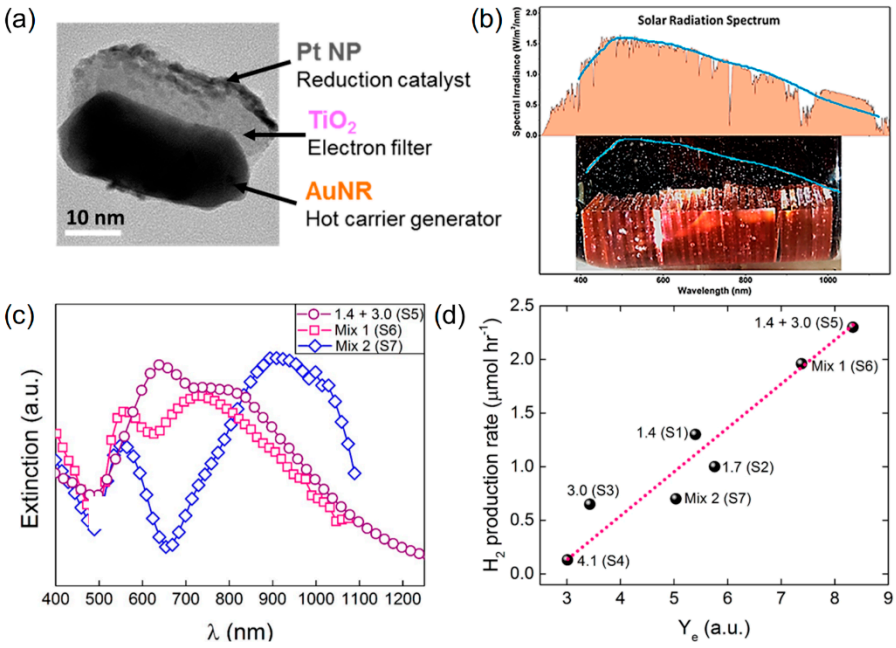

Figure 5. (**a**) Representative TEM image of an Au-TiO_2-Pt Janus particle. (**b**) A digital photograph of H_2 bubbles rising above a tandem stack of multiple plates bearing (from left to right) Janus particles of varying aspect ratios from 1.4 to 4.1 and illuminated with white light (AM 1.5). (**c**) Connection between extinction spectra and photocatalytic activity of Au-TiO_2-Pt Janus particles. (**d**) The hydrogen production rates, for the seven types of devices investigated, were plotted against a computed number proportional to the hot electron production rate. Copyright 2015 American

Peer-reviewed version available at Catalysts 2018, 8, 634; doi:10.3390/catal8120634

Chemical Society.

The arrangement of components in multi-metals/semiconductor heterojunction has a great influence on their final photocatalytic performance. Properly optimizing the structural configuration could increase the utilization efficiency of plasmon-induced hot electrons [88-90]. Meanwhile, abundant pathway of electron transfer can speed the separation of electron-hole pairs. Our previous work had certified the important role of structural arrangement for improving the photocatalytic activity [91]. We prepared an Au-Pt-CdS hetero-nanostructure, in which each component of Au, Pt, and CdS had direct contact with other two materials; Pt was on the tips and a CdS layer along the sides of an Au nanotriangle (see Figure 6a). The photocatalytic testing indicated that Au-Pt-CdS hybrids exhibited excellent photocatalytic activity for hydrogen production. Through testing the ultrafast time-resolved transient absorption (see Figure 6c), the multipathway electron-transfer processed in Au-Pt-CdS hybrids could be attested, which were illustrated in Figure 6d. The intimate and multi-interface contact between components generated multiple effective electron-transfer pathways (Au to CdS, Au to Pt, and CdS to Pt) for maximal utilization of photoexcited charges. Similar nanostructure was reported by Dong and co-workers [92]. They synthesized a ternary plasmonic photocatalyst, which featured an Au nanorod with tipped Pt nanoparticles and sided CdS nanoshells. The as-prepared Au-Pt-CdS possessed efficient UV-Vis-NIR-driven plasmonic photoactivity for hydrogen generation. The rational arrangement of the components in Au-Pt-CdS induced to plasmonic resonance energy transfer and hot electron transfer were thought be responsible for the outstanding photocatalytic activity.

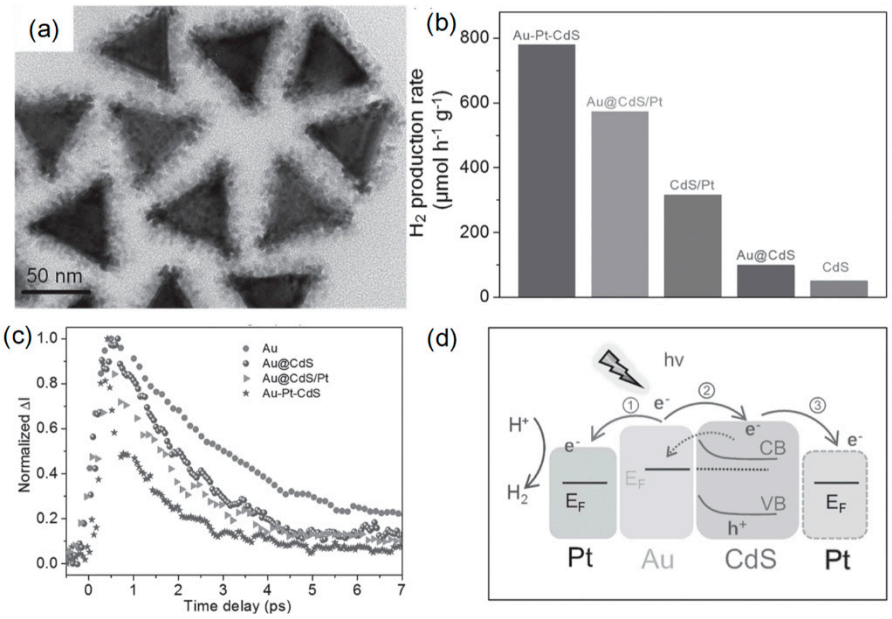

Figure 6. (**a**) TEM image of Au-Pt-CdS hetero-nanostructures. (**b**) Photocatalytic hydrogen production of contrast samples under light irradiation (λ > 420 nm). (**c**) Normalized time-resolved optical differential transmission of Au, Au@CdS, Au@CdS/Pt, and Au-CdS-Pt hetero-nanostructures. (**d**) Schematic illustration of the multipathway electron transfer in Au-Pt-CdS hetero-nanostructures. Copyright 2016 Wiley-VCH.

3. Plasmon-Mediated Heterojunctions Photocatalysis in Ternary Metal/Multi-Semiconductors Hetero-Nanostructures

Properly engineered semiconductor heterojunction photocatalysts are proved to show higher photocatalytic activity because of spatial separation of photo-generated electron-hole pairs. The direct Z-scheme and p-n heterojunctions are the most frequently studied due to their distinct advantages for charge migration [93-96]. By introduction of plasmonic metal with these junctions, the separation of electron-hole pairs could be observably expedited. In this section, we briefly review the recent works centered on plasmon-modified Z-scheme and p-n heterojunctions for efficient photocatalysis.

The Z-scheme photocatalytic concept was proposed by Bard et al. in 1979 in order to maximize the redox potential of the semiconductor heterojunction [97]. Several advantages have been obtained for Z-scheme configuration, such as effective charge separation, high reduction and oxidation power, more participant photocatalysts [98-100]. By introduce of plasmonic metals into this system, the high concentration of hot

Preprints (www.preprints.org) | NOT PEER-REVIEWED | Posted: 21 November 2018 doi:10.20944/preprints201811.0523.v1

Peer-reviewed version available at Catalysts 2018, 8, 634; doi:10.3390/catal8120634

electrons and large utilization of light induced by plasmon resonance could further promote the photocatalytic reaction [100-102]. For instance, Gao et al. fabricated a unique Au/TiO_2/WO_3 heterojunction photocatalyst for hydrogen production by a facile electrospinning technique and subsequent annealing in air [103]. In this system, plasmonic Au nanoparticles were combined with Z-scheme TiO_2/WO_3 heterojunctions (see Figure 9a-g). The hydrogen production rate of the as-prepared composite was greatly enhanced compared with pure TiO_2 (S0) and TiO_2/WO_3 (S1) (see Figure 9 h and i). In the catalytic reaction, WO_3 and Au acted as hole and electron collector, respectively. The connection of plasmonic effect and Z-scheme configuration further promoted charge separation and absorption of visible light. The synergistic effect of Schottky and plasmonic effect were thought to improve the performance of photocatalytic hydrogen production.

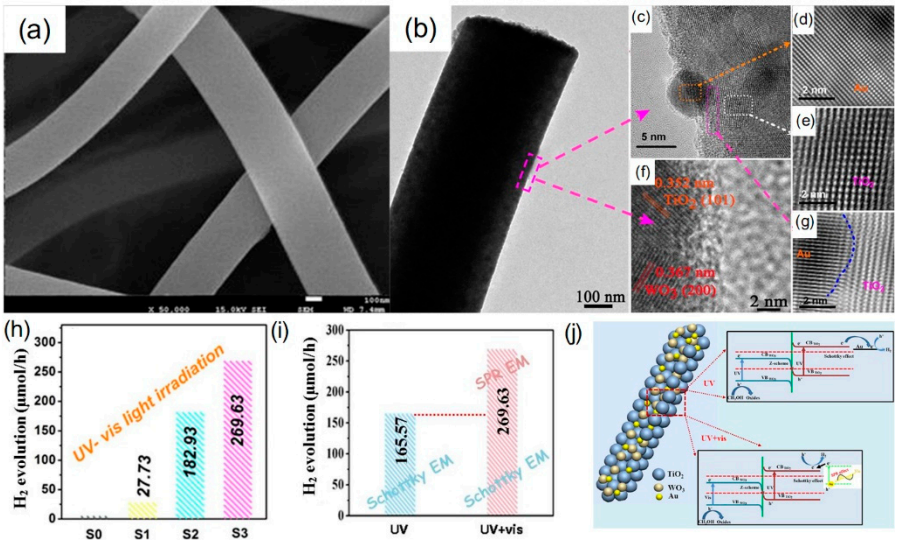

Figure 7. (**a-g**) Morphology and composition characterizations of Au/TiO_2/WO_3. (**h-i**) Photocatalytic hydrogen production activity of the contrast samples. (**J**) Schematic diagram of the photocatalytic hydrogen generation over the ternary Au/TiO_2/WO_3. Copyright 2017 Elsevier.

Meanwhile, Tang and co-workers reported a plasmon-excited dual Z-scheme system in ternary $BiVO_4$/Ag/Cu_2O nanocomposite [104]. Specifically, the nanocomposite had been synthesized via simple wet impregnation of Cu_2O particles coupled with a subsequent photo-reduction pathway for the deposition of metallic Ag on the surface of $BiVO_4$. The specific morphology of $BiVO_4$/Ag/Cu_2O was shown in Figure 8a and b. It was shown that the coating contents of the Cu_2O and Ag particles

Preprints (www.preprints.org) | NOT PEER-REVIEWED | Posted: 21 November 2018 doi:10.20944/preprints201811.0523.v1

Peer-reviewed version available at Catalysts 2018, 8, 634; doi:10.3390/catal8120634

presented a great effect on the eventual photocatalytic activity of the photocatalysts, and the optimum coating contents of Cu_2O and Ag were obtained with their mass ratios of 3% and 2%, respectively. Under optimum conditions, nearly 91.22% tetracycline removal efficiency was obtained based on ternary $BiVO_4$/Ag/Cu_2O, higher than that of pure $BiVO_4$ (42.9%) and binary $BiVO_4$/Cu_2O (65.17%) and $BiVO_4$/Ag (72.63%) nanocomposites (see Figure 8c). The enhanced photocatalytic activity was attributed to the synergistic effect of Cu_2O, Ag and $BiVO_4$, especially the surface plasmon resonance excited dual Z-scheme and established local electric field brought about by metallic Ag, which was proposed in Figure 8d.

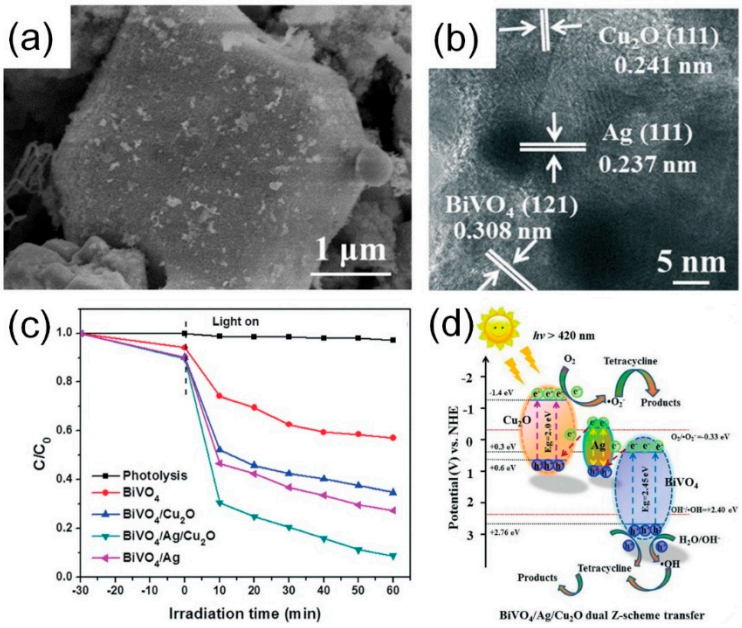

Figure 8. Morphology (**a**) and composition (**b**) characterizations of $BiVO_4$/Ag/Cu_2O composites. (**c**) The photocatalytic degradation of tetracycline based on different photocatalysts. (**d**) Schematic illustration of the proposed reaction mechanism in the $BiVO_4$/Ag/Cu_2O nanocomposite-based reaction systems towards tetracycline degradation under visible light irradiation. Copyright 2017 Royal Society of Chemistry.

The p-n heterojunction photocatalyst concept was proposed to accelerate the electron-hole migration across the heterojunction by providing an additional electric field [105-107]. Generally, an effective p-n heterojunction photocatalyst can be obtained by combining p-type and n-type semiconductors. When the p-type and n-type semiconductors are irradiated by incident light with an energy equal to or higher than

their bandgap value, both p-type and n-type semiconductors can generate electron-hole pairs. The photogenerated electrons and holes in the p-type and n-type semiconductors will migrate under the influence of the internal electric field to the conductor band of the n-type semiconductor and the valance band of the p-type semiconductor, respectively, which results in the fast-spatial separation of the electron-hole pairs [108-109]. Combing plasmonic metal nanocrystals with p-n heterojunction could further speed the separation of electron-hole pairs [110-111]. For instance, Zhou et. al fabricated a large-scale quantity of three-dimensional branched Cu_xO/ZnO@Au heterostructure consisting of CuO nanowires and grafted ZnO nanodisks decorated with Au nanoparticles via sequential hierarchical assemblies (see Figure 9a-d) [112]. The photocatalytic results indicated that Cu_xO/ZnO@Au exhibited a highest hydrogen production rate of 12.4 μmol cm^{-2} h^{-1}. The possible enhanced mechanism was proposed in Figure 9g. The synergistic effect from CuO, ZnO, and their formed intimate p-n heterojunctions extends the light absorption range and inhibits the recombination of photogenerated electron-hole pairs, as well as the strong plasmon resonance of Au were thought to be responsible for the superior photocatalytic activity.

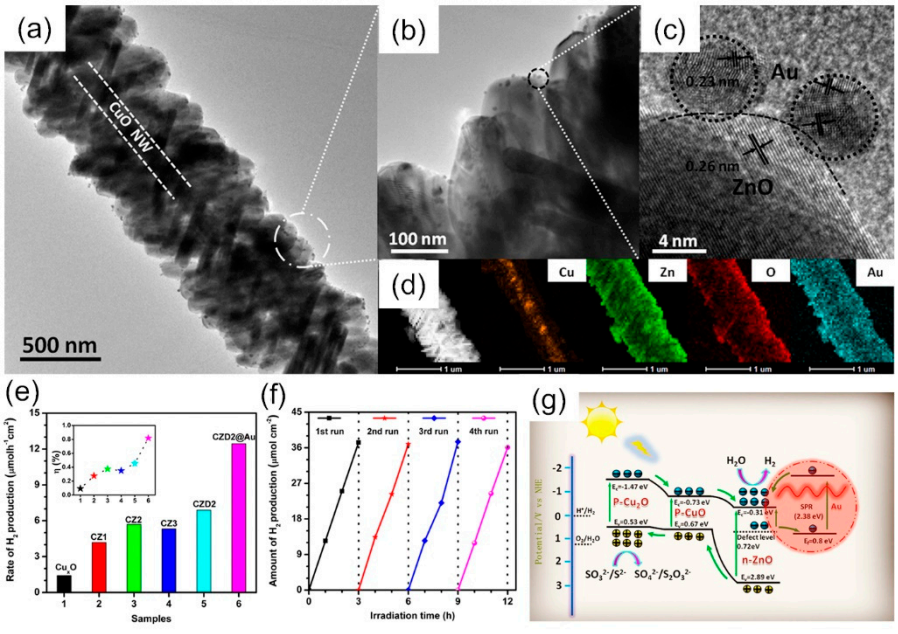

Figure 9. (**a-d**) Morphology and compositions characterizations of Cu_xO/ZnO@Au hetero-nanostructures. (**e**) Comparison of the photocatalytic hydrogen production rates over different samples under the white light irradiation. (insert) The corresponding STH conversion efficiencies.

(**f**) Recycling test of photocatalytic hydrogen production over Cu_xO/ZnO@Au. (**g**) Schematic illustration of photoexcited carrier dynamics in Cu_xO/ZnO@Au. Copyright 2015 American Chemical Society.

5. Conclusion and outlook

In recent years, the researches focused on plasmon-mediated photocatalysis of hetero-nanomaterials have been steadily expanding, the progress mentioned in this article is only a drop in the bucket. In this article, we present a concise appraisal of the recent achievements in the field of metal/semiconductor heterojunction photocatalysts, including their designs, synthesis, and photocatalytic applications. The physical mechanism for the enhanced photocatalysis in binary and ternary metal/semiconductor heterojunctions is briefly classified.

Although many exciting results have been achieved in this field, but the practical efficiency of the photocatalytic reaction is still low, the further industrialization and commercialization of the photocatalysts requires untiring explores. In our option, the future research in this field may be focused on the following aspects. Firstly, the synthetic method is the footstone for the preparation of photocatalysts. Currently, there still remains significant challenges in exploring facile, economic, environmentally friendly strategies for preparing high-performance metal/semiconductor photocatalysts. Secondly, searching new plasmonic materials and functional semiconductors to form effective heterojunctions is one of the key research goals. More research efforts should be centered on the developing new materials with low cost, high solar-conversion efficiency. Thirdly, the mechanism of plasmon-enhanced photocatalytic activity requires further systematic studies. Effective ultrafast spectral analysis technique should be applied to quantitatively verify the migration pathway of charge. Meanwhile, corresponding theoretical calculations and modeling methods for optimizing the structural construct and charge transfer should be pay more attention. Further theoretical achievement could offer a better understanding of the charge and energy transfer kinetics, then guiding the design of high-quality photocatalyst.

In brief, we have reviewed the recent progress in constructing of

metal/semiconductor photocatalyst for improved photocatalytic applications. Their photocatalytic performances varied with structural adjustment and component arrangement are demonstrated. We hope this article could inspire the further design and fabrication of functional materials used in photocatalysis and other important applications.

Acknowledgement: This study was supported by the National Natural Science Foundation of China (11804257), Natural Science Foundation of Hubei Province (2018CFB106), scientific research foundation of Wuhan Institute of Technology (18QD24 and 18QD25).

Conflicts of Interest: There are no conflicts to declare.

References

1. Chen, X., Shen, S., Guo, L., Mao, S. S. Semiconductor-based photocatalytic hydrogen generation. *Chem. Rev.* **2010**, *110*, 6503-6570.
2. Martin, D. J., Reardon, P. J. T., Moniz, S. J., Tang, J. Visible light-driven pure water splitting by a nature-inspired organic semiconductor-based system. *J. Am. Chem. Soc.* **2014**, *136*, 12568-12571.
3. Marszewski, M., Cao, S., Yu, J., Jaroniec, M. Semiconductor-based photocatalytic CO_2 conversion. *Mater. Horiz.* **2015**, *2*, 261-278.
4. Li, J., Wu, N. Semiconductor-based photocatalysts and photoelectrochemical cells for solar fuel generation: a review. *Catal. Sci. Technol.* **2015**, *5*, 1360-1384.
5. Kisch, H. Semiconductor photocatalysis-mechanistic and synthetic aspects. *Angew. Chem. Int. Ed.* **2013**, *52*, 812-847.
6. Xiang, Q., Yu, J., Jaroniec, M. Graphene-based semiconductor photocatalysts. *Chem. Soc. Rev.* **2012**, *41*, 782-796.
7. Liu, G., Jimmy, C. Y., Lu, G. Q. M., Cheng, H. M. Crystal facet engineering of semiconductor photocatalysts: motivations, advances and unique properties. *Chem. Commun.* **2011**, *47*, 6763-6783.
8. Zhang, G., Zhang, J., Zhang, M., Wang, X. Polycondensation of thiourea into carbon nitride semiconductors as visible light photocatalysts. *J. Mater. Chem.* **2012**, *22*, 8083-8091.
9. Chen, X., Liu, L., Peter, Y. Y., Mao, S. S. Increasing solar absorption for photocatalysis with black hydrogenated titanium dioxide nanocrystals. *Science* **2011**, 1200448.

10. Zhang, G., Zhang, M., Ye, X., Qiu, X., Lin, S., Wang, X. Iodine modified carbon nitride semiconductors as visible light photocatalysts for hydrogen evolution. *Adv. Mater.* **2014**, *26*, 805-809.
11. Fujishima, A., Honda, K. Electrochemical photolysis of water at a semiconductor electrode. *Nature*, **1972**, *238*, 37.
12. Fu, J., Chang, B., Tian, Y., Xi, F., Dong, X. Novel C_3N_4-CdS composite photocatalysts with organic–inorganic heterojunctions: in situ synthesis, exceptional activity, high stability and photocatalytic mechanism. *J. Mater. Chem. A* **2013**, 1(9), 3083-3090.
13. Wang, C. C., Li, J. R., Lv, X. L., Zhang, Y. Q., Guo, G. Photocatalytic organic pollutants degradation in metal-organic frameworks. *Energy Environ. Sci*. **2014**, *7*, 2831-2867.
14. Ge, L., Han, C., Liu, J. Novel visible light-induced g-C_3N_4/Bi_2WO_6 composite photocatalysts for efficient degradation of methyl orange. *Appl. Catal. B: Environ.* **2011**, *108*, 100-107.
15. Liang, Y. T., Vijayan, B. K., Gray, K. A., Hersam, M. C. Minimizing graphene defects enhances Titania nanocomposite-based photocatalytic reduction of CO_2 for improved solar fuel production. *Nano Lett.* **2011**,*11*, 2865-2870.
16. Tran, P. D., Wong, L. H., Barber, J., Loo, J. S. Recent advances in hybrid photocatalysts for solar fuel production. *Energy Environ. Sci.* **2012**, 5, 5902-5918.
17. Cowan, A. J., Durrant, J. R. Long-lived charge separated states in nanostructured semiconductor photoelectrodes for the production of solar fuels. *Chem. Soc. Rev.* **2013**, *42*, 2281-2293.
18. Müller, C. On the glass transition of polymer semiconductors and its impact on polymer solar cell stability. *Chem. Mater.* **2015**, *27*, 2740-2754.
19. Han, C., Yang, M. Q., Weng, B., Xu, Y. J. Improving the photocatalytic activity and anti-photocorrosion of semiconductor ZnO by coupling with versatile carbon. *Phys. Chem. Chem. Phys.* **2014**, *16*, 16891-16903.
20. Wu, W., Jiang, C., Roy, V. A. Recent progress in magnetic iron oxide–semiconductor composite nanomaterials as promising photocatalysts. *Nanoscale*, **2015**, *7*, 38-58.
21. Stamplecoskie, K. G., Kamat, P. V. Synergistic effects in the coupling of plasmon resonance of metal nanoparticles with excited gold clusters. *J. Phys. Chem. Lett.* **2015**, *6*, 1870-1875.
22. Juan, M. L., Righini, M., Quidant, R. Plasmon nano-optical tweezers. *Nat. Photonics* **2011**, *5*, 349.
23. Zhang, W., Huang, L., Santschi, C., Martin, O. J. Trapping and sensing 10 nm metal nanoparticles using plasmonic dipole antennas. *Nano Lett.* **2010**, 10, 1006-1011.
24. Ni, W., Kou, X., Yang, Z., Wang, J. Tailoring longitudinal surface plasmon wavelengths, scattering and absorption cross sections of gold nanorods. *ACS Nano* **2008**, *2*, 677-686.
25. Luk'yanchuk, B., Zheludev, N. I., Maier, S. A., Halas, N. J., Nordlander, P., Giessen, H., Chong, C. T. The Fano resonance in plasmonic nanostructures and metamaterials. *Nat. Mater.* **2010**, *9*, 707.

26. Aydin, K., Ferry, V. E., Briggs, R. M., Atwater, H. A. Broadband polarization-independent resonant light absorption using ultrathin plasmonic super absorbers. *Nat. Commun.* **2011**, *2*, 517.
27. Schaadt, D. M., Feng, B., Yu, E. T. Enhanced semiconductor optical absorption via surface plasmon excitation in metal nanoparticles. *Appl. Phys. Lett.* **2005**, *86*, 063106.
28. Barnes, W. L., Dereux, A., Ebbesen, T. W. Surface plasmon subwavelength optics. *Nature*, **2003**, *424*, 824.
29. Luther, J. M., Jain, P. K., Ewers, T., Alivisatos, A. P. Localized surface plasmon resonances arising from free carriers in doped quantum dots. *Nat. Mater.* **2011**, *10*, 361.
30. Schuller, J. A., Barnard, E. S., Cai, W., Jun, Y. C., White, J. S., Brongersma, M. L. Plasmonics for extreme light concentration and manipulation. *Nat. Mater.*, **2010**, *9*, 193.
31. Zijlstra, P., Paulo, P. M., Orrit, M. Optical detection of single non-absorbing molecules using the surface plasmon resonance of a gold nanorod. *Nat. Nanotechnol.* **2012**, *7*, 379.
32. Sherry, L. J., Chang, S. H., Schatz, G. C., Van Duyne, R. P., Wiley, B. J., Xia, Y. Localized surface plasmon resonance spectroscopy of single silver nanocubes. *Nano Lett.* **2005**, *5*, 2034-2038.
33. Chan, G. H., Zhao, J., Hicks, E. M., Schatz, G. C., Van Duyne, R. P. Plasmonic properties of copper nanoparticles fabricated by nanosphere lithography. *Nano Lett.* **2007**, *7*, 1947-1952.
34. Robatjazi, H., Zhao, H., Swearer, D. F., Hogan, N. J., Zhou, L., Alabastri, A., McClain, M. J., Nordlander, P., Halas, N. J. Plasmon-induced selective carbon dioxide conversion on earth-abundant aluminum-cuprous oxide antenna-reactor nanoparticles. *Nat. Commun.* **2017**, *8*, 27.
35. Orendorff, C. J., Gearheart, L., Jana, N. R., Murphy, C. J. Aspect ratio dependence on surface enhanced Raman scattering using silver and gold nanorod substrates. *Phys. Chem. Chem. Phys.* **2006**, *8*, 165-170.
36. Liao, H., Hafner, J. H. Gold nanorod bioconjugates. *Chem. Mater.* **2005**, *17*, 4636-4641.
37. Camargo, P. H., Rycenga, M., Au, L., Xia, Y. Isolating and probing the hot spot formed between two silver nanocubes. *Angew. Chem.* **2009**, *121*, 2214-2218.
38. Fu, Q., Ran, G., Xu, W. Direct self-assembly of CTAB-capped Au nanotriangles. *Nano Research* **2016**, *9*, 3247-3256.
39. Tabatabaei, M., Sangar, A., Kazemi-Zanjani, N., Torchio, P., Merlen, A., Lagugné-Labarthet, F. Optical properties of silver and gold tetrahedral nanopyramid arrays prepared by nanosphere lithography. *J. Phys. Chem. C* **2013**, *117*, 14778-14786.
40. Li, Y., Sun, J., Wang, L., Zhan, P., Cao, Z., Wang, Z. Surface plasmon sensor with gold film deposited on a two-dimensional colloidal crystal. *Appl. Phys. A* **2008**, *92*, 291-294.
41. Ma, L., Yang, D. J., Luo, Z. J., Chen, K., Xie, Y., Zhou, L., Wang, Q. Q. Controlled growth of sulfide on gold nanotriangles with tunable local field distribution and

enhanced photocatalytic activity. *J. Phys. Chem. C* **2016**, *120*, 26996-27002.

42. Ma, L., Ding, S. J. Synthesis of thermostable Au@ZnO core-shell nanorods with efficient visible-light photocatalytic activity. *Mater. Lett.* **2018**, *217*, 255-258.
43. Jiang, R., Li, B., Fang, C., Wang, J. Metal/semiconductor hybrid nanostructures for plasmon-enhanced applications. *Adv. Mater.* **2014**, *26*, 5274-5309.
44. Wang, M., Ye, M., Iocozzia, J., Lin, C., Lin, Z. Plasmon-mediated solar energy conversion via photocatalysis in noble metal/semiconductor composites. *Adv. Sci.* **2016**, *3*, 1600024.
45. Choi, W., Park, G., Bae, K. L., Choi, J. Y., Nam, K. M., Song, H. Metal–semiconductor double shell hollow nanocubes for highly stable hydrogen generation photocatalysts. *J. Mater. Chem. A* **2016**, *4*, 13414-13418.
46. Tu, W., Zhou, Y., Li, H., Li, P., Zou, Z. Au@TiO_2 yolk-shell hollow spheres for plasmon-induced photocatalytic reduction of CO_2 to solar fuel via a local electromagnetic field. *Nanoscale*, **2015**, *7*, 14232-14236.
47. Linic, S., Aslam, U., Boerigter, C., Morabito, M. Photochemical transformations on plasmonic metal nanoparticles. *Nat. Mater.* **2015**, *14*, 567.
48. Zhang, Y., He, S., Guo, W., Hu, Y., Huang, J., Mulcahy, J. R., Wei, W. D. Surface-plasmon-driven hot electron photochemistry. *Chem. Rev.* **2017**, *118*, 2927-2954.
49. Bernardi, M., Mustafa, J., Neaton, J. B., Louie, S. G. Theory and computation of hot carriers generated by surface plasmon polaritons in noble metals. *Nat. Commun.* **2015**, *6*, 7044.
50. Hong, T., Chamlagain, B., Hu, S., Weiss, S. M., Zhou, Z., Xu, Y. Q. Plasmonic hot electron induced photocurrent response at MoS_2-metal junctions. *ACS Nano* **2015** *9*, 5357-5363.
51. Li, W., Valentine, J. G. Harvesting the loss: surface plasmon-based hot electron photodetection. *Nanophononics*, **2017**,*6*, 177.
52. Li, J., Cushing, S. K., Meng, F., Senty, T. R., Bristow, A. D., Wu, N. Plasmon-induced resonance energy transfer for solar energy conversion. *Nat. Photonics* **2015**, *9*, 601.
53. Wu, K., Chen, J., McBride, J. R., Lian, T. Efficient hot-electron transfer by a plasmon-induced interfacial charge-transfer transition. *Science*, **2015**, 349, 632-635.
54. Ma, X. C., Dai, Y., Yu, L., Huang, B. B. Energy transfer in plasmonic photocatalytic composites. *Light-Sci. Appl.* **2016**, *5*, e16017.
55. Brongersma, M. L., Halas, N. J., Nordlander, P. Plasmon-induced hot carrier science and technology. *Nat. Nanotechnol.* **2015**, *10*, 25.
56. Li, M., Yu, X. F., Liang, S., Peng, X. N., Yang, Z. J., Wang, Y. L., Wang, Q. Q. Synthesis of Au-CdS core-shell hetero-nanorods with efficient exciton-plasmon interactions. *Adv. Funct. Mater.* **2011**, *21*, 1788-1794.
57. Ma, L., Liang, S., Liu, X. L., Yang, D. J., Zhou, L., Wang, Q. Q. Synthesis of dumbbell-like gold-metal sulfide core-shell nanorods with largely enhanced transverse plasmon resonance in visible region and efficiently improved photocatalytic activity. *Adv. Funct. Mater.* **2015**, *25*, 898-904.
58. Zhang, J., Tang, Y., Lee, K., Ouyang, M. Nonepitaxial growth of hybrid core-shell

nanostructures with large lattice mismatches. *Science*, **2010**, *327*, 1634-1638.

59. Lu, B., Liu, A., Wu, H., Shen, Q., Zhao, T., Wang, J. Hollow Au-Cu_2O core-shell nanoparticles with geometry-dependent optical properties as efficient plasmonic photocatalysts under visible light. *Langmuir*, **2016**, *32*, 3085-3094.
60. Li, B., Gu, T., Ming, T., Wang, J., Wang, P., Wang, J., Yu, J. C. (Gold core)@(ceria shell) nanostructures for plasmon-enhanced catalytic reactions under visible light. *ACS Nano*, **2014**, *8*, 8152-8162.
61. Muhammed, M. A. H., Döblinger, M., Rodríguez-Fernández, J. Switching plasmons: gold nanorod-copper chalcogenide core-shell nanoparticle clusters with selectable metal/semiconductor NIR plasmon resonances. *J. Am. Chem. Soc.* **2015**, *137*, 11666-11677.
62. Liu, J., Feng, J., Gui, J., Chen, T., Xu, M., Wang, H., Dong, H., Chen, H., Li, X., Wang, L., Chen, Z., Yang, Z., Liu, J., Hao, W., Yao, Y., Gu, Y., Weng, Y., Huang, Y., Duan, X., Zhang, J., Li Y. Metal@ semiconductor core-shell nanocrystals with atomically organized interfaces for efficient hot electron-mediated photocatalysis. *Nano Energy* **2018**, *48*, 44-52.
63. Feng, J., Liu, J., Cheng, X., Liu, J., Xu, M., Zhang, J. Hydrothermal cation exchange enabled gradual evolution of Au@ZnS-AgAuS yolk-shell nanocrystals and their visible light photocatalytic applications. *Adv. Sci.* **2018**, *5*, 1700376.
64. Chang, Y., Cheng, Y., Feng, Y., Jian, H., Wang, L., Ma, X., Li, X., Zhang, H. Resonance energy transfer-promoted photothermal and photodynamic performance of gold-copper sulfide yolk-shell nanoparticles for chemophototherapy of cancer. Nano letters, **2018**, *18*, 886-897.
65. Ji, M., Li, X., Wang, H., Huang, L., Xu, M., Liu, J., Liu, J., Wang, J., Zhang, J. Versatile synthesis of yolk/shell hybrid nanocrystals via ion-exchange reactions for novel metal/semiconductor and semiconductor/semiconductor conformations. *Nano Research* **2017**, *10*, 2977-2987.
66. Wan, G., Peng, X., Zeng, M., Yu, L., Wang, K., Li, X., Wang, G. The Preparation of Au@TiO_2 yolk-shell nanostructure and its applications for degradation and detection of methylene blue. *Nanoscale Research Lett.* **2017**, *12*, 535.
67. Lee, S. U., Jung, H., Wi, D. H., Hong, J. W., Sung, J., Choi, S. I., Han, S. W. Metal–semiconductor yolk-shell heteronanostructures for plasmon-enhanced photocatalytic hydrogen evolution. *J. Mater. Chem. A* **2018**, 6(9), 4068-4078.
68. Costi, R., Cohen, G., Salant, A., Rabani, E., Banin, U. Electrostatic force microscopy study of single Au-CdSe hybrid nanodumbbells: evidence for light-induced charge separation. *Nano Lett.* **2009**, *9*, 2031-2039.
69. Chakrabortty, S., Yang, J. A., Tan, Y. M., Mishra, N., Chan, Y. Asymmetric dumbbells from selective deposition of metals on seeded semiconductor nanorods. *Angew. Chem.* **2010**, *122*, 2950-2954.
70. Kim, Y., Park, K. Y., Jang, D. M., Song, Y. M., Kim, H. S., Cho, Y. J., Myung, Y., Park, J. Synthesis of Au-Cu_2S core- shell nanocrystals and their photocatalytic and electrocatalytic activity. *J. Phys. Chem. C* **2010**, 114, 22141-22146.
71. Wu, B., Liu, D., Mubeen, S., Chuong, T. T., Moskovits, M., Stucky, G. D. Anisotropic growth of TiO_2 onto gold nanorods for plasmon-enhanced hydrogen

production from water reduction. *J. Am. Chem. Soc.* **2016**, *138*, 1114-1117.

72. Hong, J. W., Wi, D. H., Lee, S. U., Han, S. W. Metal-semiconductor heteronanocrystals with desired configurations for plasmonic photocatalysis. *J. Am. Chem. Soc.* **2016**, *138*, 15766-15773.
73. Tsukamoto, D., Shiro, A., Shiraishi, Y., Sugano, Y., Ichikawa, S., Tanaka, S., Hirai, T. Photocatalytic H_2O_2 production from ethanol/O_2 system using TiO_2 loaded with Au-Ag bimetallic alloy nanoparticles. *ACS Catal.* **2012**, *2,* 599-603.
74. Zhou, N., Polavarapu, L., Gao, N., Pan, Y., Yuan, P., Wang, Q., Xu, Q. H. TiO_2 coated Au/Ag nanorods with enhanced photocatalytic activity under visible light irradiation. *Nanoscale* **2013**, *5*, 4236-4241.
75. Li, Y., Zhang, B. P., Zhao, J. X. Enhanced photocatalytic performance of Au-Ag alloy modified ZnO nanocomposite films. *J. Alloys Compd.* **2014**, *586*, 663-668.
76. Kamimura, S., Yamashita, S., Abe, S., Tsubota, T., Ohno, T. Effect of core@shell (Au@Ag) nanostructure on surface plasmon-induced photocatalytic activity under visible light irradiation. *Appl. Catal. B: Environ.* **2017**, *211*, 11-17.
77. Zielińska-Jurek, A., Kowalska, E., Sobczak, J. W., Lisowski, W., Ohtani, B., Zaleska, A. Preparation and characterization of monometallic (Au) and bimetallic (Ag/Au) modified-Titania photocatalysts activated by visible light. *Appl. Catal. B: Environ.* **2011**, *101*, 504-514.
78. Tahir, M., Tahir, B., Amin, N. A. S. Synergistic effect in plasmonic Au/Ag alloy NPs co-coated TiO_2 NWs toward visible-light enhanced CO_2 photoreduction to fuels. *Appl. Catal. B: Environ.* **2017**, *204*, 548-560.
79. Zhai, H., Wang, P., Zhang, Q., Liu, X., Wang, Z., Liu, Y., Zheng, Z., Huang, B. Plasmonic Au-Ag bimetallic alloy nanoparticles decorated ZnO nanorod with enhanced photocatalytic activity for ethylene-oxidation. *Appl. Catal. A: General* **2018**, doi.org/10.1016/j.apcata.2018.06.019.
80. Kamimura, S., Miyazaki, T., Zhang, M., Li, Y., Tsubota, T., Ohno, T. (Au@Ag)@Au double shell nanoparticles loaded on rutile TiO_2 for photocatalytic decomposition of 2-propanol under visible light irradiation. *Appl. Catal. B: Environ.* **2016**, *180*, 255-262.
81. Zheng, Z., Tachikawa, T., Majima, T. Single-particle study of Pt-modified Au nanorods for plasmon-enhanced hydrogen generation in visible to near-infrared region. *J. Am. Chem. Soc.* **2014**, *136*, 6870-6873.
82. Li, K., Hogan, N. J., Kale, M. J., Halas, N. J., Nordlander, P., Christopher, P. Balancing near-field enhancement, absorption, and scattering for effective antenna-reactor plasmonic photocatalysis. *Nano Lett.* **2017**, *17*, 3710-3717.
83. Yu, L., Shao, Y., Li, D. Direct combination of hydrogen evolution from water and methane conversion in a photocatalytic system over Pt/TiO_2. *Appl. Catal. B: Environ.* **2017**, *204*, 216-223.
84. Xue, J., Ma, S., Zhou, Y., Zhang, Z., He, M. Facile photochemical synthesis of Au/Pt/g-C_3N_4 with plasmon-enhanced photocatalytic activity for antibiotic degradation. *ACS Appl. Mater. Interface* **2015**, *7*, 9630-9637.
85. Wang, F., Jiang, Y., Lawes, D. J., Ball, G. E., Zhou, C., Liu, Z., Amal, R. Analysis of the promoted activity and molecular mechanism of hydrogen production over

fine Au-Pt alloyed TiO_2 photocatalysts. *ACS Catal.* **2015**, *5*, 3924-3931.

86. Zhang, Z., Li, A., Cao, S. W., Bosman, M., Li, S., Xue, C. Direct evidence of plasmon enhancement on photocatalytic hydrogen generation over Au/Pt-decorated TiO_2 nanofibers. *Nanoscale* **2014**, *6*, 5217-5222.
87. Mubeen, S., Lee, J., Liu, D., Stucky, G. D., Moskovits, M. Panchromatic photoproduction of H_2 with surface plasmons. *Nano Lett.* **2015**, *15*, 2132-2136.
88. Tanaka, A., Hashimoto, K., Kominami, H. Visible-light-induced hydrogen and oxygen formation over $Pt/Au/WO_3$ photocatalyst utilizing two types of photoabsorption due to surface plasmon resonance and band-gap excitation. *J. Am. Chem. Soc.* **2014**, *136*, 586-589.
89. She, P., Xu, K., Zeng, S., He, Q., Sun, H., Liu, Z. Investigating the size effect of Au nanospheres on the photocatalytic activity of Au-modified ZnO nanorods. *J. Colloid. Interface Sci.* **2017**, *499*, 76-82.
90. Yun, J., Hwang, S. H., Jang, J. Fabrication of Au@Ag core/shell nanoparticles decorated TiO_2 hollow structure for efficient light-harvesting in dye-sensitized solar cells. *ACS Appl. Mater. Interface* **2015**, *7*, 2055-2063.
91. Ma, L., Chen, K., Nan, F., Wang, J. H., Yang, D. J., Zhou, L., Wang, Q. Q. Improved hydrogen production of Au-Pt-CdS hetero-nanostructures by efficient plasmon-induced multipathway electron transfer. *Adv. Funct. Mater.* **2016**, *26*, 6076-6083.
92. Wu, J., Zhang, Z., Liu, B., Fang, Y., Wang, L., Dong, B. UV-Vis-NIR-driven plasmonic photocatalysts with dual-resonance modes for synergistically enhancing h_2 generation. *Solar RRL*, **2018**, *2*, 1800039.
93. Xia, P., Zhu, B., Cheng, B., Yu, J., Xu, J. 2D/2D $g\text{-}C_3N_4/MnO_2$ nanocomposite as a direct Z-scheme photocatalyst for enhanced photocatalytic activity. *ACS Sustain. Chem. Eng.* **2017**, *6*, 965-973.
94. Zhou, P., Yu, J., Jaroniec, M. All-solid-state Z-scheme photocatalytic systems. *Adv. Mater.* **2014**, *26*, 4920-4935.
95. Maeda, K. Z-scheme water splitting using two different semiconductor photocatalysts. *ACS Catal.* **2013**, *3*, 1486-1503.
96. Chen, Z., Wang, W., Zhang, Z., Fang, X. High-efficiency visible-light-driven Ag3PO4/AgI photocatalysts: Z-scheme photocatalytic mechanism for their enhanced photocatalytic activity. *J. Phys. Chem. C* **2013**, *117*, 19346-19352.
97. Bard, A. J. Photoelectrochemistry and heterogeneous photo-catalysis at semiconductors. *J. Photochem.* **1979**, *10*, 59-75.
98. Jia, Q., Iwase, A., Kudo, A. $BiVO_4$-Ru/$SrTiO_3$: Rh composite Z-scheme photocatalyst for solar water splitting. *Chem. Sci.* **2014**, *5*, 1513-1519.
99. Zhou, F. Q., Fan, J. C., Xu, Q. J., Min, Y. L. $BiVO_4$ nanowires decorated with CdS nanoparticles as Z-scheme photocatalyst with enhanced H_2 generation. *Appl. Catal. B: Environ.* **2017**, *201*, 77-83.
100. Jin, J., Yu, J., Guo, D., Cui, C., Ho, W. A Hierarchical Z-scheme CdS-WO_3 photocatalyst with enhanced CO_2 reduction activity. *Small*, **2015**, *11*, 5262-5271.
101. Ye, L., Liu, J., Gong, C., Tian, L., Peng, T., Zan, L. Two different roles of metallic Ag on Ag/AgX/BiOX (X = Cl, Br) visible light photocatalysts: surface plasmon resonance and Z-scheme bridge. *ACS Catal.* **2012**, *2*, 1677-1683.

102. Zhang, J., Niu, C., Ke, J., Zhou, L., Zeng, G. Ag/AgCl/Bi_2MoO_6 composite nanosheets: A plasmonic Z-scheme visible light photocatalyst. *Catal. Commun.* **2015**, *59*, 30-34.
103. Gao, H., Zhang, P., Zhao, J., Zhang, Y., Hu, J., Shao, G. Plasmon enhancement on photocatalytic hydrogen production over the Z-scheme photosynthetic heterojunction system. *Appl. Catal. B: Environ.* **2017**, *210*, 297-305.
104. Deng, Y., Tang, L., Zeng, G., Feng, C., Dong, H., Wang, J., Feng, H., Liu, Y., Zhou, Y., Pang, Y. Plasmonic resonance excited dual Z-scheme $BiVO_4$/Ag/Cu_2O nanocomposite: synthesis and mechanism for enhanced photocatalytic performance in recalcitrant antibiotic degradation. *Environm. Sci. Nano* **2017**, *4*, 1494-1511.
105. Jiang, D., Chen, L., Zhu, J., Chen, M., Shi, W., Xie, J. Novel p-n heterojunction photocatalyst constructed by porous graphite-like C_3N_4 and nanostructured BiOI: facile synthesis and enhanced photocatalytic activity. *Dalton Trans.* **2013**, *42*, 15726-15734.
106. Chen, C., Cai, W., Long, M., Zhou, B., Wu, Y., Wu, D., Feng, Y. Synthesis of visible-light responsive graphene oxide/TiO_2 composites with p/n heterojunction. *ACS Nano* **2012**, *4*, 6425-6432.
107. Zhang, Z., Shao, C., Li, X., Wang, C., Zhang, M., Liu, Y. Electrospun nanofibers of p-type NiO/n-type ZnO heterojunctions with enhanced photocatalytic activity. *ACS Appl. Mater. Interface* **2010**, *2*, 2915-2923.
108. Peng, Y., Yan, M., Chen, Q. G., Fan, C. M., Zhou, H. Y., Xu, A. W. Novel one-dimensional Bi_2O_3-Bi_2WO_6 p-n hierarchical heterojunction with enhanced photocatalytic activity. *J. Mater. Chem. A* **2014**, *2*, 8517-8524.
109. Lin, L., Yang, Y., Men, L., Wang, X., He, D., Chai, Y., Zhao, B., Ghoshroy, S., Tang, Q. A highly efficient TiO_2@ZnO n-p-n heterojunction nanorod photocatalyst. *Nanoscale*, **2013**, 5(2), 588-593.
110. Zhao, W., Dai, B., Zhu, F., Tu, X., Zhang, L., Li, S., Leung, D. Y. C., Cheng, S. A novel 3D plasmonic p-n heterojunction photocatalyst: Ag nanoparticles on flower-like p-Ag_2S/n-$BiVO_4$ and its excellent photocatalytic reduction and oxidation activities. *Appl. Catal. B: Environ.* **2018**, *229*, 171-180.
111. Pal, J., Sasmal, A. K., Ganguly, M., Pal, T. Surface plasmon effect of Cu and presence of n-p heterojunction in oxide nanocomposites for visible light photocatalysis. *J. Phys. Chem. C* **2015**, *119*, 3780-3790.
112. Zhou, G., Xu, X., Ding, T., Feng, B., Bao, Z., Hu, J. Well-steered charge-carrier transfer in 3D branched Cu_xO/ZnO@Au heterostructures for efficient photocatalytic hydrogen evolution. *ACS Appl. Mater. Interface* **2015**, *7*, 26819-26827.